Punctual ecological changes rather than global factors drive species diversification and the evolution of wing phenotypes in *Morpho* butterflies.

Nicolas Chazot[1,*], Patrick Blandin[2], Vincent Debat[2], Marianne Elias[2], Fabien L. Condamine[3]

[1] *Department of Ecology, Swedish University of Agricultural Sciences, Ulls väg 16 75651 Uppsala, Sweden.*

[2]*Institut de Systématique, Évolution, Biodiversité, ISYEB - UMR 7205 – CNRS MNHN UPMC EPHE, Muséum national d'Histoire naturelle, Sorbonne Universités, 57 rue Cuvier CP50 F-75005, Paris, France.*

[3]*CNRS, UMR 5554 Institut des Sciences de l'Evolution (Université de Montpellier), Place Eugène Bataillon, 34095 Montpellier, France.*

Corresponding author (*):

Nicolas Chazot, email: chazotn@gmail.com.

Acknowledgments

The authors have no conflict of interest to declare. F.L.C. has benefited from an "Investissements d'Avenir" grant managed by Agence Nationale de la Recherche (CEBA, ref. ANR-10-LABX-25-01). P.B benefited from the Programme Pluriformation "Etat et structure phylogénétique de la biodiversité actuelle et fossile".

Abstract

Assessing the relative importance of geographical and ecological drivers of evolution is paramount to understand the diversification of species and traits at the macroevolutionary scale. Here, we use an integrative approach, combining phylogenetics, biogeography, ecology, and quantified phenotypes to investigate the drivers of both species and phenotypic diversification of the iconic Neotropical butterfly genus *Morpho*. We generated a time-calibrated phylogeny for all known species and inferred historical biogeography. We fitted models of time-dependent (accounting for rate heterogeneity across the phylogeny) and paleoenvironment-dependent diversification (accounting for global effect on the phylogeny). We used geometric morphometrics to assess variation of wing size and shape across the tree, and investigated their dynamics of evolution. We found that the diversification of *Morpho* is best explained when considering multiple independent diversification dynamics across the tree, possibly associated with lineages occupying different microhabitat conditions. First, a shift from understory to canopy was characterized by an increased speciation rate partially coupled with an increasing rate of wing shape evolution. Second, the occupation of dense bamboo thickets accompanying a major host-plant shift from dicotyledons towards monocotyledons was associated with a simultaneous diversification rate shift and an evolutionary "jump" of wing size. Our study points to a diversification pattern driven by punctual ecological changes instead of a global driver or biogeographic history.

Keywords

Species diversification, phenotypic diversification, wing size, wing shape, geometric morphometrics, butterflies, *Morpho.*

Introduction

Investigating the rates of phenotypic evolution and the relationships between phenotypes and species ecology can shed light on the drivers of time and geographic patterns of diversity. Previous studies have demonstrated that rates of both species and phenotypic diversification vary widely through time and among clades at all taxonomic scales (e.g. Venditti *et al.*, 2011; Eastman *et al.*, 2011; Rabosky & Adams, 2012; Rabosky *et al.*, 2013; Rabosky *et al.*, 2014; Cooney & Thomas, 2020). These variations have resulted in the striking heterogeneity in species and phenotypic diversity observed across the tree of life. Such variations may eventually be coupled, indicating an interaction between the processes of species and phenotypic diversifications. Studies investigating such coupling have yielded contrasted results. Some of them support an association between specific and phenotypic diversification (e.g. in salamanders: Rabosky & Adams, 2012; fish: Rabosky *et al.*, 2013; vertebrates: Cooney & Thomas, 2020), while others found no support for this relationship (e.g. in lizards: Rabosky *et al.*, 2014; squirrels: Zelditch *et al.*, 2015; reef fishes: Price *et al.*, 2015; snakes: Lee *et al.*, 2016). For example in squirrels, Zelditch *et al.* (2015) suggested that species diversification was geographically driven while phenotypic diversification was ecologically driven, resulting in a decoupling of the two dynamics.

A correlation between species and phenotypic diversification rates is notably expected in some specific cases. For example, adaptive radiations – rapid adaptive diversification in a variety of ecological niches – are expected to produce bursts of diversification and phenotypic evolution especially during the initial stages of diversification (Schluter, 2000; Gavrilets & Losos, 2009). Speciation rate increases when a large number of ecological niches are vacant while phenotypes rapidly evolve in response to the diversity of ecological opportunities. Strong correlation between speciation rates and phenotypic diversification may also be found when the focal trait directly drives reproductive isolation. For example, the

evolution of male genitalia, involved in mating, may facilitate reproductive isolation between populations (see Langerhans *et al.*, 2016 for a review). Correlated dynamics leading to a lower rate of diversification can also be predicted. For example, if extinction probability is biased with respect to phenotype leading to a non-random loss of variation in a particular clade, both species and morphological diversity should show a correlated drop down (Foote, 1997). In this study, we assess the role of multiple ecological causes of variations in rates of species and wing diversification and the extent to which these variations are coupled, by focusing on the case of the butterfly genus *Morpho* (Nymphalidae).

The genus *Morpho* comprises 30 species (Blandin & Purser, 2013), which are amongst the largest butterflies in the Neotropics and are well known for their blue iridescent wing coloration. Several ecological factors have already been suggested as potential drivers of diversification and phenotypic evolution. Previous biogeographic estimations suggested that *Morpho* butterflies originated and started diversifying in the Andes (Penz *et al.*, 2012, Blandin & Purser 2013), before spreading across the Neotropics. There is also evidence that *Morpho* lineages separated early in their history into two microhabitats (DeVries *et al.*, 2010; Chazot *et al.*, 2016). One clade is composed of species that tend to fly high, often above the forest canopy, with some species typically harbouring gliding flight behaviour such as *M. cisseis* and *M. hecuba*. The remaining species mostly fly within the first meters above ground in the understory (DeVries *et al.*, 2010; Chazot *et al.*, 2016). Finally, according to Cassildé *et al.* (2010) and Penz *et al.* (2012), the genus *Morpho* was ancestrally feeding on monocotyledons, and two major host-plant shifts occurred during its diversification: after the first divergence event, one of the two clades shifted to dicotyledon host-plants and, within this clade, a subclade subsequently reversed to the monocotyledons.

Here we focus on the wings of *Morpho*, which are at the crossroad of multiple selective pressures and tightly linked to species diversification. Typically, wing colour

patterns can be involved in camouflage, aposematism or courting behaviours (Naisbit *et al.*, 2001; Merrill *et al.*, 2011). Wings also allow flight, enabling dispersal, foraging, predator escape, mating or host-plant searching (Dudley, 2002). Hence butterfly wings are under strong natural and/or sexual selection and may be associated with variations of speciation rate (Ortiz-Acevedo *et al.*, 2020). Both size and shape are important aspects of wing morphology. They both strongly affect the performance of flight behaviours (Dudley, 2002; Le Roy *et al.*, 2019) and therefore might be closely associated to habitat use, dispersal strategies or host-plant searching. Besides, fore and hind wings can be functionally differentiated, for example during flight (Grodnitsky *et al.*, 1994; Le Roy *et al.*, 2020), which may lead to uncorrelated patterns of diversification.

To investigate whether species and phenotypic diversification dynamics are coupled and to identify potential drivers of variations, we inferred a time-calibrated molecular phylogeny of the genus that we combined to a dataset of geographical distributions and morphometric measurements of wing size and shape. We applied an integrative approach and addressed the following questions: (1) Have rates of phenotypic diversification varied across the tree? We investigated potential variations in rate of phenotypic diversification among clades using phenograms and models of trait evolution to compare evolutionary rates for wing size and shape. (2) Is species diversification better explained by global processes or clade-specific (ecological) factors? First, we fitted different models of species diversification testing for global drivers of diversification, specifically past temperatures and Andean orogeny. Second, we compared these global drivers to models in which species diversification varied according to clade-specific ecological factors (microhabitat and major shifts of host-plants) and/or variations of phenotypic diversification identified in the first step. (3) Can we explain the variations in diversification rates by historical biogeography? We performed ancestral areas estimation in order to assess whether variations in phenotypic

evolutionary rates or species diversification rates may be associated with specific biogeographic events.

Material and methods

Time-calibrated phylogeny

Phylogenetic relationships and divergence time were inferred with Bayesian inference. We concatenated DNA data for one mitochondrial (COI) and four nuclear genes (CAD, EF-1α, GAPDH and MDH) using published sequences (Cassildé *et al.*, 2012; Penz *et al.*, 2012; Chazot *et al.*, 2016) retrieved from GenBank, generating a molecular dataset of a total length of 5001 nucleotides. Our dataset includes all *Morpho* species (i.e. 30 species *sensu* Blandin, 2007). *Morpho helenor*, which harbours many subspecies, is distributed throughout the entire Neotropical region, resulting in unresolved biogeographic reconstructions in preliminary analyses. To help resolving the biogeographic inferences, *M. helenor* was represented in the biogeographic analyses by six subspecies that each occupies a distinct Neotropical area. For all other analyses, we pruned all subspecies of *M. helenor* but one in order to keep a single branch for the species. We also included 11 outgroups to root and calibrate the tree (see Supporting Information S1) on the basis of the most comprehensive nymphalid phylogeny to date (Wahlberg *et al.*, 2009).

To simultaneously estimate the topology and branching times of the phylogeny we used a Bayesian relaxed-clock approach as implemented in *BEAST* 1.8.2 (Drummond *et al.*, 2012). To choose the best partitioning strategy and the corresponding substitution models, we ran *PartitionFinder* 1.1.1 (Lanfear *et al.*, 2012) allowing all possible partitions and models implemented in *BEAST*. Three subsets were defined: the first included position 1 and 2 of all genes and followed a GTR+I+Γ model, the second included position 3 of all nuclear fragments and followed a GTR+Γ model, and the third including the position 3 of the

147 mitochondrial fragment and followed a TrN+Γ model. We implemented an uncorrelated
148 lognormal relaxed clock model. Given the lack of *Morpho* fossil we relied on secondary
149 calibrations to calibrate the molecular clock. Penz *et al.* (2012) calibrated the divergence
150 between *Morpho* and its sister groups using a unique calibration point from Wahlberg *et al.*
151 (2009), and a normal distribution for the corresponding prior. However, Sauquet *et al.* (2012)
152 showed that using a single secondary calibration prior could yield biased estimates. Hence,
153 we used a set of seven calibrations defined by uniform priors bounded by the 95% credibility
154 intervals (95% CI) estimated by Wahlberg *et al.* (2009) (see Supporting Information S1). We
155 implemented a Yule process for the tree prior, and we ran the phylogenetic analyses for 30
156 million Markov chain Monte Carlo (MCMC) generations. We checked for chain convergence
157 using *Tracer* 1.6, as indicated by effective sample size (ESS) values. Finally, we used
158 *TreeAnnotator* 1.8.2 (Drummond *et al.*, 2012) to select the maximum clade credibility (MCC)
159 tree with median age values calculated from the posterior distribution of branch lengths,
160 applying a 20% burn-in.
161
162 ***Morphological data***
163 Our morphological dataset (published by Chazot *et al.* 2016) consists in the size and shape of
164 the fore and hind wings, as assessed by morphometric measurements. A total of 911
165 collection specimens of both sexes and representing all *Morpho* species were photographed.
166 Wing shape was described using landmarks and semi-landmarks placed at vein intersections
167 and wing margins, respectively (see Chazot *et al.*, 2016 for details), which were
168 superimposed with *tpsRelw* (Rohlf, 1993). Wing size was measured using the log-
169 transformed mean centroid size per species. Importantly, for analyses involving wing shape
170 we used the residuals of a multivariate regression of species mean Procrustes coordinates on
171 species mean centroid size (log-transformed), which allows focusing on the non-allometric

shape variation. Similar analyses were performed separately on the fore and hind wings. All analyses were performed on males and females separately. As we found divergent patterns among sexes, we show the results for males and females separately. No female *M. niepelti* was available. This species was therefore pruned from the tree for all analyses involving female data.

Dynamics of phenotypic diversification

We investigated whether the evolutionary rates of wing size and shape have varied among subclades across the phylogeny.

Wing size – We first visualized the evolution of traits through time using the *phenogram* function in *PHYTOOLS* 0.5-20 (Revell, 2012), which represents the trait values inferred at each node along a time axis. Second, we investigated the dynamics of wing size evolution across lineages using the method implemented in the function *rjmcmc.bm* available in *GEIGER* 2.0.6 (Harmon *et al.*, 2008; Eastman *et al.*, 2011) for univariate traits. This method uses Bayesian analyses and reversible-jump MCMC to infer the number and the location of shifts of morphological diversification dynamics. We fitted and compared three different models of trait evolution: (1) a single-rate Brownian model (BM); (2) a relaxed model of Brownian evolution in which a trait evolved according to distinct Brownian-motion models across the tree (rBM); and (3); a model in which trait evolution can also occur at punctual "jumps", i.e. brief periods of rapid evolution at any branch in the phylogeny (jBM). We ran models on both the MCC and a posterior distribution of trees. For the MCC tree analysis, we ran for each model one MCMC of 30 million generations, sampling every 3,000 generations. We checked for convergence of each run using *CODA (*Plummer *et al.* 2020*)*, and computed the ESS. We applied a 25% burn-in and compared the three models using the Akaike's Information Criterion for MCMC samples *aicm* and *aicw* implemented in *GEIGER*

(Supporting Information S2). To assess the robustness of the inferences to branch length uncertainties, we repeated the analysis on a posterior distribution of trees and summarized the results. We sampled 100 trees with a topology identical to that of the MCC tree from the posterior distribution. For each tree, we ran the three models but reduced the MCMC to 10 million generations, calculated the *aicm* score, the mean *aicm* pairwise differences between models and the position of rate shifts and jumps. We summarized the results by calculating the frequency of shifts and jumps at nodes across the posterior distribution. These results are hereafter referred to as shift/jump posterior tree frequencies.

Wing shape –Some authors have used the scores on the first PC-axis as a univariate shape measure (e.g. Rabosky *et al.*, 2014; Thacker, 2014) to investigate shifts in evolutionary rates for multidimensional traits, but this may lead to spurious results (Uyeda *et al.*, 2014). We rather investigated variations in rates of shape evolution across the phylogeny in a multivariate way using the function *compare.evol.rate* from *GEOMORPH* (Adams, 2014; Denton & Adams, 2015). It allows testing whether species assigned to different ecological factors have significantly different rates of shape evolution, by comparing the ratio between the rates of each group to a null distribution of ratios obtained through simulation of a unique neutral evolutionary rate (two or more factors can be tested). When more than two factors are included, the function performs a global test for the significance of the multiple rates model compared to a one-rate model, but also assesses the significance of differences among each pair of factors. We used this factor assignment to define monophyletic subgroups with potentially divergent evolutionary rate from the background rate. We first tested all models with one shift, i.e. all species belonging to one subclade (each subclade had a minimum of three species) are assigned to one group, and the rest of the species assigned to another group. If two or more subclades were identified as having a rate of evolution significantly different from that of the background, we identified the subclade with the highest ratio (hence the

greatest shift). Then we ran again *compare.evol.rate* on all possible combinations of two shifting subclades that include the first identified shift. A two-shift model was considered significant if at least the two shifting subclades showed a significant difference with the background rate when considering the pairwise comparisons. Given the relatively small size of our phylogeny, we limited our analysis to two shifts (Supporting Information S3-S4). As for wing size, we repeated the analysis on both the MCC tree and a posterior distribution of trees with identical topologies. We summarized the results from the posterior distribution by calculating the frequency of significant shifts at nodes across the trees, and refer to these as posterior tree frequencies.

Dynamics of species diversification

We compared two types of species diversification models: (1) diversification rates varying according to global factors, i.e. factors virtually affecting all lineages, and (2) diversification rates varying at specific clades characterized by clade-specific ecological factors. For each type we investigated different factors (see below). All models were compared using their AIC scores to identify the model that best explains the diversification of the genus *Morpho*.

Global drivers of diversification – We tested the role of temperature fluctuations and of the paleo-elevation of the Andes on species diversification by using birth-death models that allow speciation and extinction rates to vary according to a past environmental variable itself varying through time (Condamine *et al.*, 2013). For each paleoenvironmental variable, we designed three models to be tested: *(i)* the speciation rate varies exponentially with the environment and the extinction rate is constant, *(ii)* the speciation rate is constant and the extinction rate varies exponentially with the environment, and *(iii)* both speciation and extinction rates vary exponentially with the environment. We repeated these three models with a linear dependence to the environmental variable, instead of exponential dependence.

247 For temperature we relied on the well-known Cenozoic temperature dataset published by
248 Zachos *et al.* (2008). The orogeny of the Andes is a highly complex process, with important
249 differences in uplift tempo and mode from the south of Central Andes to Northern Andes
250 (Blandin & Purser, 2013, and references therein). Several general phases have been identified
251 from the late Eocene to present, but they are difficult to synthetize in a unique model. As
252 Blandin & Purser (2013) suggested that the early diversification of the *Morpho* occurred
253 along the proto-Central Andes, we used the model of surface uplift inferred by Leier *et al.*
254 (2013) for the eastern cordillera of the southern Central Andes to test the possible influence
255 of Andean orogeny on the diversification of the *Morpho*. We used the R-package *PSPLINE*
256 1.0-17 to reconstruct smooth lines of the paleo-data for each environmental variable. The
257 smooth line is introduced in the birth-death model to represent the variation of the
258 environment through time. Given the dated phylogeny, the model then estimates speciation
259 and extinction rates, as well as their respective variations according to the environment
260 (Condamine *et al.*, 2013). These analyses were performed on 200 trees randomly sampled
261 from the posterior distribution generated by BEAST.

262 *Clade-specific drivers of diversification* – We assessed whether the diversification
263 rates across the genus *Morpho* have varied among specific clades using models of time-
264 dependent diversification. To do so we used the method developed by Morlon *et al.* (2011),
265 which allows partitioning diversification rates into independent dynamics (a backbone and
266 different subclades). We compared different partitioning schemes according to three events:
267 (1) the microhabitat change (from understory to canopy), (2) the shift of wing shape
268 evolutionary rate, and (3) the reverse shift to monocotyledon host-plants (also identified as a
269 punctual evolutionary jump of wing size at the stem). Because the evolutionary rate shift of
270 wing shape is nested within the microhabitat shift (see Results), we could not test both
271 combined. Instead, each of those shifts was combined to the monocotyledon host-plant shift

with a two-shift model of diversification rate. For each subclade and the remaining backbone, we fitted the following models: *(i)* constant speciation rate and no extinction, *(ii)* time-dependent speciation rate and no extinction, *(iii)* constant speciation and extinction rates, *(iv)* time-dependent speciation rate and constant extinction rate, *(v)* constant speciation rate and time-dependent extinction rate, and *(vi)* time-dependent speciation and extinction rates. Time dependency was modelled using an exponential function of time. The stem branch of each subclade was included in the subclades and excluded from the backbones but we kept the node of the divergence (speciation event) of the subclade within the backbones. The root of the tree was excluded from the analyses. The analysis was performed on the MCC tree, since partitioning the tree requires defining clades *a priori*, which entails a fixed topology.

Historical biogeography

To assess where and when diversification occurred, we estimated ancestral areas using the dispersal-extinction-cladogenesis (DEC, Ree and Smith, 2008) model as implemented in the R-package *BioGeoBEARS* 0.2.1 (Matzke, 2014). The analyses were performed using the MCC tree (outgroups removed) and included six subspecies of *M. helenor* (each subspecies was assigned to its current distribution).

The distribution of *Morpho* is restricted to South America and Central America (all Neotropics except the Caribbean Islands). A geographic model was incorporated to include operational areas, defined as geographic ranges shared by at least two or more species and delimited by geological, oceanic or landscape features, which may have acted as barriers to dispersal. The model comprised 7 component areas: (A) Central America, (B) trans-Andean South-America, (C) slopes of northern Andes, (D) eastern slopes of central Andes, Orinoco-Amazonian basin north of the Amazon, including the Guyanas, (E) Amazonian basin, south of the Amazon River, and (F) Atlantic forest.

297 An adjacency matrix was designed whilst taking into account the geological history
298 and the biological plausibility of combined ranges (Supporting Information S6).
299 Distributional data were compiled from monographies (Blandin, 2007). We excluded
300 distribution margins overlapping with adjacent areas. For example, *M. marcus* and *M.*
301 *eugenia* are mainly found in lowlands but their distributions reach the Andean slopes up to
302 altitudes of 700-800m. Nevertheless, we did not consider these as species occupying the
303 Andean biogeographic areas. By contrast, a species such as *M. sulkowskyi*, which occurs
304 between 1500 and 3500m high in the Andes was considered as an Andean species. We also
305 set a maximum of 3 areas per node to be constitutive of an ancestral range. We fitted two
306 different DEC models, one that assumed equal dispersal probabilities among all areas and one
307 that included time-stratified matrices of varying dispersal probabilities (Supporting
308 Information S6). We compared the likelihoods of both reconstructions to select the model
309 best explaining the current pattern of species distribution.
310
311 **Results**
312 ***Divergence times***
313 We estimated that the genus *Morpho* diverged (stem age) from its sister genus *Caerois* 38.05
314 Ma (95% CI=35.48-39.20 Ma) and the first event (crown age) of diversification was
315 recovered at 28.12 Ma (95% CI=25.22-31.24 Ma; Supporting Information S1). These
316 divergence time estimates are slightly older than those estimated by Penz *et al.* (2012) and
317 Chazot et al. (2019) who found an average divergence from *Caerois* around 32.00 Ma and
318 29.08 Ma respectively. This difference probably results from prior choices for calibrating the
319 trees (see Material and Methods).
320
321 ***Dynamics of phenotypic diversification***

322 *Wing size* – Both analyses on the MCC and posterior distribution of trees found
323 similar results. We found no support for any shift in rate of wing size diversification.
324 However, we found support for an evolutionary jump. For females the model jBM was highly
325 supported for both wings, with a highly probable (posterior tree frequency [PF] of 0.99,
326 Supporting Information S2) evolutionary jump at the root of the clade including the species
327 *M. absoloni*, *M. aurora*, *M. zephyritis*, *M. rhodopteron*, *M. sulkowskyi*, *M. lympharis*, *M.*
328 *aega*, and *M. portis* (subclade portis). Phenograms show that in this subclade, female wings
329 are on average 34% smaller than in the other *Morpho* species for both fore and hind wings
330 (Fig. 1). This is all the more striking as the sister clade (including *M. amathonte*, *M.*
331 *menelaus*, and *M. godartii*) contains some of the largest species of the genus (e.g. *M.*
332 *amathonte* has a wingspan of 10–15 cm). For males, the *portis* clade exhibits the same trend,
333 but the support for the evolutionary jump is lower than for females ($PF_{forewing}$=0.76,
334 $PF_{hindwing}$=0.71, respectively, Supporting Information S2). Males wings in the portis clade
335 were on average 30 and 32% smaller for fore and hind-wing respectively.
336 *Wing shape* – We found support for two shifts of evolutionary rate for male hindwing,
337 in both cases towards lower rate of evolution. These subclades encompass *M. helenor*, *M.*
338 *achilles*, and *M. granadensis* (Fig. 2, Supporting Information S3) on one side, and *M.*
339 *godartii*, *M. menelaus*, and *M. amathonte* on the other. This result was supported by the
340 analyses with the MCC tree. The analyses performed on the posterior tree distribution found
341 a moderate support for these shifts, with PF of 0.62 and 0.77, respectively. For females and
342 for both wings the subclade encompassing *M. theseus*, *M. amphitryon*, *M. telemachus* and *M.*
343 *hercules* exhibited the greatest shift (highest ratio) (Fig. 2, Supporting Information S4). This
344 shift corresponds to a large increase in rate of evolution (forewing ratio=181.74, hindwing
345 ratio=184.49 in the MCC analysis), i.e. wing shape evolving faster within this group than the

346 other *Morpho*. This result was strongly supported by posterior distribution analyses, with PF
347 of 0.96 and 0.99 for fore and hind-wing, respectively.
348
349 ***Dynamics of species diversification***
350 *Global drivers of diversification* – In the best model accommodating for Central
351 Andean paleo-altitudes, speciation rates were negatively dependent on the paleo-altitude and
352 extinction rates were constant (Table 2a). This model leads to a continuous decrease in
353 speciation rate towards the present, suggesting that *Morpho* diversification was high during
354 the early stages of the orogeny but the rise in altitude did not lead to any increased
355 opportunities for speciation over time. We also found a significant correlation between
356 *Morpho* diversification and temperature compared to a null model (Table 2b). The best fitting
357 paleoclimatic model indicates that speciation rate was positively correlated with temperature
358 variation while extinction remained constant. This means that speciation rate was high during
359 the initial stages of diversification when the temperatures were warmer but globally
360 decreased during the last 14 million years as the Earth cooled down (Zachos *et al.*, 2008).
361 *Clade-specific dynamics of diversification* – The best-partitioned models included a
362 shift of diversification rate for the host-plant shift and for the canopy shift (Table 3,
363 Supporting Information S5). Under this configuration, the diversification of the clade that
364 shifted to monocotyledon host-plants was best modelled by a speciation rate decreasing
365 through time combined with no extinction, and the diversification of the canopy clade was
366 best modelled by a constant speciation rate with no extinction (Table 3, Fig. 3). For the
367 remaining backbone lineages the best fitting model was a time-dependent speciation and
368 extinction. The resulting net diversification rate (speciation minus extinction) of this
369 backbone was high during the very early stages of diversification but rapidly decreased
370 through time and became negative *ca.* 25 Ma, implying a declining diversity (Fig. 3). Around

22 Ma, the net diversification rate became positive again and reached zero at the present. This model of partitioned dynamics of diversification outperformed any model involving a global driver of diversification. Indeed, the multi-rate time-dependent model better fit the diversification of *Morpho* (AICc=191.69) than the temperature-dependent model (AICc=197.3, ΔAIC=5.61) and the altitude-dependent model (AICc=199.0, ΔAIC=7.31).

Historical biogeography

The model of biogeographic estimation with user-specified dispersal probabilities yielded a worse fit than the model with equal dispersal probabilities (likelihood with time-stratified dispersal multipliers: DEC_{strat}=-143.41; likelihood without time-stratified dispersal multipliers DEC_{null}=-140.75) and the ancestral state estimations involved some important differences. In both reconstructions the root state was highly unresolved. In the DEC_{null} model (highest likelihood), the area with the highest probability at the root was the southern part of the Amazonian Basin, *ca.* 28.1 Ma. The early divergence of the clade containing *M. marcus* and *M. eugenia* was accompanied by a colonization of the northern part of the Amazonian Basin (Fig. 4). The ancestor of the remaining group of *Morpho* occupied the Central Andes. This lineage then diverged into an Andean and an Amazonian lineage. This event (21.8 Ma) was also accompanied by a shift in microhabitat use: flight in low forest strata (understory) for the Andean lineage, and flight high above ground up to the canopy for the Amazonian lineage. The Andean lineage began a long-term occupation of the Central Andes with local diversification (12 nodes inferred occupying the Central Andes after the initial dispersal event). Around 11-12 Ma, cis-Andean (east of the Andes) recolonizations of Amazonia and the Atlantic Forest happened in three lineages. *M. polyphemus* is an intriguing case as it diverged 20.8 Ma from an Andean ancestor, but nowadays occupies Central America, whose connection to South America is often considered to be only completed

396 during the last 4-3 million years. This implies either an earlier dispersal route of emerging
397 Central America or a more recent dispersal with a joint extinction in the South American
398 landmass. Overall, Northern Amazonia and the Northern Andes appear to have been
399 colonized recently, during the last 5 million years (Fig. 4).
400
401 **Discussion**
402 In this study we aimed at investigating the large-scale patterns of diversification of the
403 *Morpho* butterflies by jointly evaluating the dynamics of species and phenotypic
404 diversification, to assess whether they are coupled or not and to test whether they correlate
405 with clade-specific factors and/or biogeographic events. Our results show that ecological
406 idiosyncrasies predominantly explain the pattern of diversification, instead of global (tree
407 wide) factors. These ecological changes affected to a large extent both species and
408 phenotypic diversification, leading to the partial coupling of both dynamics. Based on the
409 amount of information currently available on the ecology of *Morpho* we discuss the potential
410 role of several ecological and biogeographic events as well as the correlation with phenotypic
411 diversification in explaining these variations among groups.
412
413 *Study limitations*
414 A number of limitations have to be mentioned before discussing our results. Focusing on a
415 small clade allowed us to combine multiple ecological, morphological and historical
416 components thereby providing a deep understanding of the *Morpho* history. Although we
417 sampled all known species for both the molecular phylogeny and morphological traits, our
418 comparative analyses probably lack power as a result of both the small number of taxa (30
419 species) and the phylogenetic distribution of the traits of interest. Both microhabitat shift and
420 host-plant shift (towards monocotyledons) are single events happening at the root of a single

421 clade each and we lack phylogenetically independent similar shifts. Typically, we found an
422 evolutionary jump in wing size to be associated with a shift from dicotyledons to
423 monocotyledons host-plants. Further work addressing this pattern at a larger phylogenetic
424 scale will be necessary to assess the generality of our finding. Furthermore, the reliability of
425 birth-death models to assess the diversification dynamics from phylogenies of extant taxa is
426 debated (e.g. Quental & Marshall, 2010; Louca & Pennell, 2020). We thus remain cautious
427 with our estimation of the diversification dynamics and the interpretation of the different
428 models tested. In particular, we avoided interpreting the speciation and extinction rates
429 independently to focus only on the net diversification dynamics. Finally, the timing and
430 magnitude of the Andean surface uplift is also controversial (see for example Evenstar *et al.*,
431 2015, and references therein; Fiorella *et al.*, 2015). We based our test on the reconstruction
432 proposed by Leier *et al.* (2013) that focused only on the eastern cordillera of the Central
433 Andes where the *Morpho* diversity is the highest, but had a large uncertainty in their paleo-
434 altitude estimations. The Andean orogeny was spatially and temporally heterogeneous
435 (Horton, 2018), which makes the use and interpretation of the paleoaltitude-dependent
436 diversification model difficult (Condamine *et al.*, 2018). Those limitations should thus be
437 kept in mind throughout the following discussion of the drivers of diversification, and the
438 signal of declining diversity in particular.
439
440 *Early Andean diversification not directly driven by Andean uplift*
441 The diversification of the genus *Morpho* in the Andes could have happened either
442 simultaneously with the uplift – a scenario where speciation is driven by the increasing
443 heterogeneity of ecological conditions with new altitudes (Lagomarsino *et al.*, 2016) – or
444 decoupled from orogenesis – a scenario where a clade radiates across a range of altitudes
445 already established through adaptations to ecological conditions (e.g. climate, host-plants,

446 predators). Our results support the second hypothesis. We found that a model of
447 diversification rate responding to paleo-altitude performed worse than the clade-specific
448 diversification models (Tables 2 and 3), which means that neither global speciation nor
449 extinction rate variations are well explained by the paleo-altitudes of the Central Andes. From
450 a biogeographic point of view, 16 extant species (over 30) are almost restricted to the
451 lowlands, while only six extant species have a distribution strictly restricted to the Andes.
452 Yet, from the Oligocene-Miocene boundary to middle Miocene periods (23.5 to 11.6 Ma), 11
453 nodes out of 14 were inferred to be at least in the Central Andes from our biogeographic
454 estimation (Fig. 4). Combined to the hypothesis that the *Morpho* probably originated in the
455 foothills of the proto-Central-Andes, it is undeniable that the Central Andes played an
456 important role in the early diversification of *Morpho*. During the second half of their
457 evolutionary history, these lineages dispersed and diversified out of the Central Andes.

458 In contrast with the pattern of Central Andean diversification described above, the
459 Northern Andes appear to have played only a minor role: while Northern Andean uplift likely
460 established a barrier in three instances, resulting in cis- and trans-Andean *Morpho* lineages
461 (Fig. 4), no major diversification was associated with the periods of Northern Andean uplift
462 (Blandin & Purser, 2013). This absence of local diversification in the Northern Andes is a
463 major difference compared to other butterflies such as the Ithomiini in which several groups
464 repeatedly diversified at a high rate in the Northern Andes such as the genera *Napeogenes*
465 (Elias *et al.*, 2009), *Oleria* (De-Silva *et al.*, 2016), *Hypomenitis* (Chazot *et al.*, 2016) or
466 *Pteronymia* (De-Silva *et al.*, 2017).

467 Diversification driven by host-plant evolution may be an alternative explanation for
468 the early diversification of *Morpho*. Penz and DeVries (2002) and Cassildé *et al.* (2010)
469 suggested that monocotyledons were the ancestral host-plants of the genus *Morpho*, probably
470 because at the time it was admitted that *M. marcus* larvae feed on monocotyledons

(Constantino, 1997). However, we now know that *M. marcus* very probably feeds on Fabaceae (e.g. *Inga auristellae*; Ramírez-Garcia *et al*., 2014; Vásquez Bardales *et al.*, 2017), and *M. eugenia* certainly feed on Caesalpiniaceae (Bénéluz, 2016). Therefore, since groups closely related to *Morpho*, notably the sister genus *Caerois*, are known to only feed on monocotyledon host-plants (Beccaloni *et al*., 2008), it is likely that the divergence of the *Morpho* was associated with an initial shift to dicotyledons. This host-plant shift at the root of Morphos created the conditions for an early rapid diversification of the group.

A shift towards the canopy driving phenotypic and diversification changes

We found a shift of species diversification associated with a single shift from the understory to the canopy (DeVries *et al.* 2010; Chazot *et al*. 2016). We also found strong indications that female wing shape evolution in the canopy clade is different from a neutral evolution. An increasing rate of shape evolution for both fore- and hind-wings was supported in the subclade nested in the canopy clade and including *M. theseus*, *M. niepelti*, *M. amphytrion*, *M. telemachus*, and *M. hercules*. Chazot *et al*. (2016) showed that both male and female wing shapes in the canopy clade are significantly different from wing shapes in understory species. Here we show that this microhabitat change associated with different vegetation structure, microclimatic conditions and predator community may have also affected the rate of female wing shape evolution in addition to shape *per se*. However, we note that the highest rate shift was not placed at the root of the canopy clade, suggesting that other factors may have caused this rapid phenotypic evolution. This increased rate of wing shape evolution was not found in males. Instead, in males we found two significant slowdowns in rate at different small subclades, only in the case of hindwings. The lack of more precise information on these species ecology unfortunately prevents speculating on the factors involved in such changes in wing shape evolutionary rate.

A second change in microhabitat conditions associated with a host-plant, phenotypical and diversification shifts

Published information in the *portis* clade (Heredia & Alvarez, 2007; Beccaloni *et al.*, 2008; Montero Abril & Ortiz Perez, 2010) indicate that four *Morpho* species (*M. portis, M. aega*, *M. sulkowskyi* and *M. rhodopteron*) feed on Neotropical woody bamboos (Poaceae, tribe Bambuseae), notably on *Chusquea* species (subtribe Chusqueinae), in particular *Chusquea* aff. *scandens* for *M. sulkowskyi* that occurs at cloud forest elevations (Heredia & Alvarez, 2007). Recent observations indicate that M. zephyritis also feeds on woody bamboos (Roberto Maravi, pers. comm.). For the other species of the *portis* clade, there are only field observations indicating that they live in areas with important bamboo vegetation (Purser & Lacomme, 2016; pers. obs. in Peru, Daniel Lacomme pers. com.).

If, as observations indicate, the *portis* clade diversified after an initial shift back to monocotyledon host-plants, this reversal evolutionary event is a strong support for the "oscillation hypothesis" (Janz *et al.*, 2006). This hypothesis was proposed to explain the pattern of nymphalid butterflies with respect to host-plant use (Janz *et al.*, 2006) and states that the ability to recolonize "lost" hosts should be conserved over long evolutionary times, leading to recurrent recolonization events. Compared to the speciation rate of the backbone, species diversification within the *portis* clade proceeded at a higher rate, and rapidly decreased through time to reach almost zero at present. Adaptive radiations, here following a major host-plant shift, predict this rapid dampening of speciation rate as a result of niche filling (Schluter, 2000; Gavrilets & Losos, 2009).

Interestingly, we found that an evolutionary jump – a fast punctual event of evolution – toward smaller wing sizes also coincided with the host-plant shift. Chazot *et al.* (2016) did not identify any driver of this wing size evolution. To our knowledge, there is no clear

521 expectation or evidence supporting a specific relationship between body size and monocot
522 *versus* dicot feeders but this question has rarely been addressed (but see Garcia-Barros 2000).
523 The jump toward smaller sizes also cannot be associated with any altitudinal change because
524 some species of the clade only occur at low to mid altitudes (200-1500 m), while others occur
525 at higher altitudes (1500-3500 m) (Blandin, 2007; Gayman *et al*., 2016).

526 Therefore, other hypotheses need to be explored, in particular that of a second
527 possible change of microhabitat conditions. Many Bambusinae, in particular *Chusquea*
528 species, form dense thickets, twigs and leaves creating inextricable tangles as a result from
529 abundant vegetative branching at each node (Fisher, 2011; Fisher *et al*., 2014). Observational
530 data on the behaviour of the bamboo feeding *Morpho* is scarce, but observations on *M.*
531 *rhodopteron* (Montero Abril and Ortiz Perez, 2010; Purser and Lacomme, 2016), *M.*
532 *sulkowskyi* (Heredia and Alvarez-Lopez 2007), and *M. aega* (Otero & Marigo, 1990) suggest
533 that females are more often resting inside the *Chusquea* thickets while males are flying
534 around (males, when resting, also stand in the vegetation). Moreover, Heredia & Alvarez-
535 Lopez (2007) noted that *M. sulkowskyi* females having light and dark alternating stripes on
536 wings ventral side are difficult to detect inside *Chusquea* thickets. More or less contrasted
537 similar patterns exist in males and females of other species, except in *M. absoloni*. Therefore,
538 we hypothesize that size reduction, associated to a more or less striped appearance of the
539 ventral side, could be an adaptation to the microhabitat structure of dense woody bamboo
540 thickets, highlighting once again the importance of the microhabitat conditions on species
541 and trait evolution.

542

543 *Declining diversity in the Neotropical* Morpho

544 When accounting for heterogeneity in diversification rates (isolating the two shifting
545 subclades), the diversification dynamics for the remaining lineages was characterized by a

546 negative net diversification rate, indicative of a declining diversity, mainly during the
547 Miocene. Whether diversity decline can be accurately estimated only from phylogenies of
548 extant species is a matter of debate (e.g. Quental & Marshall, 2010; but see Morlon *et al.*,
549 2011). In the case of *Morpho*, this pattern may explain why some branches in the tree (such
550 as the stem branch of *M. marcus* and *M. eugenia* or the branches leading to *M. anaxibia*, *M.*
551 *deidamia*, or *M. polyphemus*) are surprisingly long. Extinct lineages may also explain why *M.*
552 *polyphemus*, which diverged from its sister clade 20 Ma, is found in Central America, while
553 colonization of Central America is often expected to be much more recent (but see Montes *et*
554 *al.*, 2015, Farris *et al.*, 2011). Major landscape transformations during the Miocene in western
555 Amazonia may explain this decline. Between 23-10 Ma, Western Amazonia transformed into
556 a large wetland of lakes, swamps and shallow water, called the Pebas System (Wesselingh
557 *et al.*, 2001; Hoorn *et al.*, 2010). The exact nature of the Pebas System is still under
558 discussion but it was most likely unsuitable for terrestrial fauna (Salas-Gismondi *et al.*,
559 2015). Evidence of extinction has been found from a west Amazonian fossil record, in
560 particular with a major decrease of mammalian diversity at the transition between the
561 Oligocene and the Miocene (Antoine *et al.*, 2016), which is in line with the beginning of the
562 diversity decline in *Morpho* (Fig. 3).
563
564 *Conclusion*
565 Our results support a prevailing ecological basis for both species and phenotypic
566 diversification in *Morpho* butterflies: (1) a major host-plant shift, which punctually affected
567 wing size evolution and greatly affected species diversification dynamics (pattern of adaptive
568 radiation), and (2) a microhabitat shift affecting species diversification and partially wing
569 shape diversification. Therefore, to a large extent, the dynamics of species diversification and
570 phenotypic diversification are coupled in *Morpho*, most likely as a result of two major

571 ecological events. More importantly, we show that both species and phenotypic
572 diversification in *Morpho* butterflies are better explained by multiple clade-specific factors
573 instead of global abiotic drivers. Current methods for identifying drivers of diversification,
574 based on model comparisons, are unable to test for potential interactions between drivers.
575 Hence, our results do not exclude the possibility that the Andes played a role in
576 diversification, but rather suggest that their effect on the shape of the phylogenetic tree was
577 less significant than other factors. Nevertheless, the extent to which the effects of these
578 ecological drivers can be generalised is unknown given the scale of our dataset. In particular
579 future work at a larger phylogenetic scale should shed light on the importance of major host-
580 plant transitions on the evolution of body size and the dynamics of diversification. Our study
581 also highlights that both phenotypic and ecological information are of key relevance for
582 understanding macroevolutionary patterns of diversification.
583
584

585 **Table 1.** Summary results obtained from fitting three models of trait evolution on 100 trees,
586 using the *rjmcmc.bm* function as implemented in the R package GEIGER on a) males and b)
587 females. *bm*=single Brownian rate, *rbm*=relaxed Brownian rates, *jbm*=jumps of Brownian
588 rates. AICbm, AICrbm, AICjbm = mean AIC score across the 100 trees for all three models.
589 ΔAIC bm-rbm, ΔAIC bm-jbm, ΔAIC rbm-jbm = pairwise AIC differences between models for each
590 tree.

591

592 **a) Males**

	AICbm	AICrbm	AICjbm	ΔAIC bm-rbm	ΔAIC bm-jbm	ΔAIC rbm-jbm
Forewing	-23.92 (18.72)	-27.78 (10.33)	13.41 (26.32)	3.85 (21.70)	-37.34 (34.54)	-41.20 (30.02)
Hindwing	-14.43 (20.28)	-18.62 (14.58)	14.94 (24.28)	4.18 (24.02)	-29.37 (29.76)	-33.56 (28.21)

593

594 **b) Females**

	AICbm	AICrbm	AICjbm	ΔAIC bm-rbm	ΔAIC bm-jbm	ΔAIC rbm-jbm
Forewing	-22.36 (10.44)	-17.74 (9.40)	-34.70 (1.60)	-4.61 (15.73)	12.33 (10.98)	16.95 (9.56)
Hindwing	-15.44 (17.06)	-13.30 (22.83)	-32.80 (1.17)	-2.14 (29.62)	17.36 (16.88)	19.50 (23.01)

Table 2. Paleoenvironmental-dependent diversification analyses using paleoaltitude (a) and Cenozoic temperature (b) data. Mean parameter and standard error estimates are presented for each model. Best-fitting model, as determined via a combination of the lowest AIC and ΔAIC (see main text) highlighted in bold. In our best-fit paleoaltitude-dependent model, speciation is negatively correlated to Andean orogeny over time (adding extinction as a parameter did not improve the model fit). Likewise, speciation is positively correlated to temperature variation over time (allowing extinction to vary with temperature did not improve the likelihood). λ = speciation rate (in events/Myr/lineage); μ = extinction rate (in events/Myr/lineage); α = rate of variation of the speciation according to the relevant paleoenvironmental variable; β = rate of variation of the extinction according to the paleoenvironmental variable; NP = number of parameters in each model.

a) Paleoaltitude models

Models	Dependency	NP	logL	AIC	ΔAIC	λ	α	μ	β
λ Alti. and no μ	Linear	2	-97.50 ±0.085	199.00 ±0.171	0.00	0.190 ±0.004	-3.60E-05 ±1.39E-06	-	-
λ Alti. and no μ	Exponential	2	-97.68 ±0.083	199.37 ±0.166	0.37	0.210 ±0.004	-3.06E-04 ±5.76E-06	-	-
λ Alti and μ constant.	Linear	3	-97.49 ±0.085	200.99 ±0.170	1.99	0.190 ±0.0003	-3.47E-05 ±8.75E-07	5.15E-04 ±4.17E-04	-
λ Alti. and μ constant	Exponential	3	-97.69 ±0.083	201.37 ±0.166	2.37	0.220 ±0.004	-3.11E-04 ±5.68E-06	9.09E-07 ±7.91E-07	-
λ constant and μ Alti	Exponential	3	-97.75 ±0.104	201.51 ± 0.207	2.51	0.080 ±3.16E-04	-	42038.92 ±11873.33	-7.48E-03 ±2.62E-04
λ Alti. and μ Alti	Exponential	4	-96.94 ±0.094	201.87 ±0.187	2.87	0.880 ±0.160	-5.00E-04 ±2.00E-05	6.820 ±1.159	-1.89E-03 ±4.72E-05
λ Alti. and μ Alti.	Linear	4	-97.42 ±0.086	202.83 ±0.171	3.84	0.210 ±0.004	-3.83E-05 ±1.18E-06	0.070 ±0.007	-2.38E-05 ±2.32E-06
λ constant and μ Alti.	Linear	3	-98.56 ±0.099	203.12 ±0.198	4.12	0.080 ±0.001	-	0.030 ±0.005	-1.14E-05 ±1.76E-06

b) Paleoclimate models

Models	Dependency	NP	logL	AIC	ΔAIC	λ	α	μ	β
λ Temp. and no μ	Exponential	2	-96.65 ±0.095	197.30 ±0.189	0.00	0.030 ±4.13E-04	0.179 ±1.91E-03	-	-
λ Temp. and no μ	Linear	2	-96.72 ±0.097	197.44 ±0.195	0.13	0.015 ±5.50E-04	0.013 ±1.17E-04	-	-
λ Temp and μ constant	Exponential	3	-96.58 ±0.092	199.15 ±0.184	1.85	0.030 ±3.93E-04	0.210 ±3.62E-03	0.043 ±0.004	-
λ Temp. and μ constant	Linear	3	-96.67 ±0.097	199.33 ±0.195	2.03	0.023 ±1.48E-03	0.021 ±1.34E-03	0.046 ±0.007	-
λ Temp. and μ Temp.	Linear	4	-96.42 ±0.095	200.85 ±0.189	3.54	0.017 ±1.11E-03	0.027 ±8.07E-04	0.290 ±0.012	-0.037 ±0.002
λ Temp. and μ Temp	Exponential	4	-96.55 ±0.092	201.10 ±0.183	3.80	0.032 ±7.99E-04	0.205 ±4.57E-03	0.156 ±0.040	-0.164 ±0.019
λ constant and μ Temp.	Exponential	3	-98.57 ±0.103	203.14 ±0.205	5.84	0.081 ±2.96E-04	-	4.47E-08 ±3.08E-09	0.004 ±2.19E-04
λ constant and μ Temp.	Linear	3	-98.57 ±0.103	203.14 ±0.205	5.84	0.081 ±2.97E-04	-	1.09E-04 ±1.08E-04	-1.37E-05 ±1.37E-05

615 **Table 3.** Results of model comparison for the five time-dependent diversification analyses
616 presented, with mean parameter estimates for each model. λ = speciation rate (in
617 events/Myr/lineage); α = parameter of rate variation for speciation; μ = extinction rate (in
618 events/Myr/lineage); β = parameter of rate variation for extinction; NP = number of
619 parameters in each model; AICc = corrected Akaike information criterion; logL = log-
620 likelihood.

621

Clade partition	Models	NP	logL	AIC	λ	α	μ	β	Joint logL	Joint AIC
background	BVAR DVAR	4	-35.68	79.36	0.063	0.237	0.079	0.228		
monocots	BVAR	2	-21.78	47.55	0.014	0.213	-	-	-88.84	191.69
canopy	BCST	1	-31.39	64.77	0.083	-	-	-		
background	BCST	1	-50.91	103.83	0.072	-	-	-		
monocots	BVAR	2	-21.78	47.55	0.014	0.213	-	-	-92.83	193.66
shape shift	BCST	1	-20.14	42.28	0.095	-	-	-		
background	BCST	1	-73.75	149.49	0.081	-	-	-	-95.52	197.05
monocots	BVAR	2	-21.78	47.55	0.014	0.213	-	-		
whole	BCST	1	-98.40	198.81	0.081	-	-	-	-98.40	198.81
background	BCST	1	-78.18	158.36	0.078	-	-	-	-98.32	200.63
shape shift	BCST	1	-20.14	42.28	0.095	-	-	-		
background	BCST	1	-67.01	136.03	0.080	-	-	-	-98.40	200.80
canopy	BCST	1	-31.39	64.77	0.083	-	-	-		

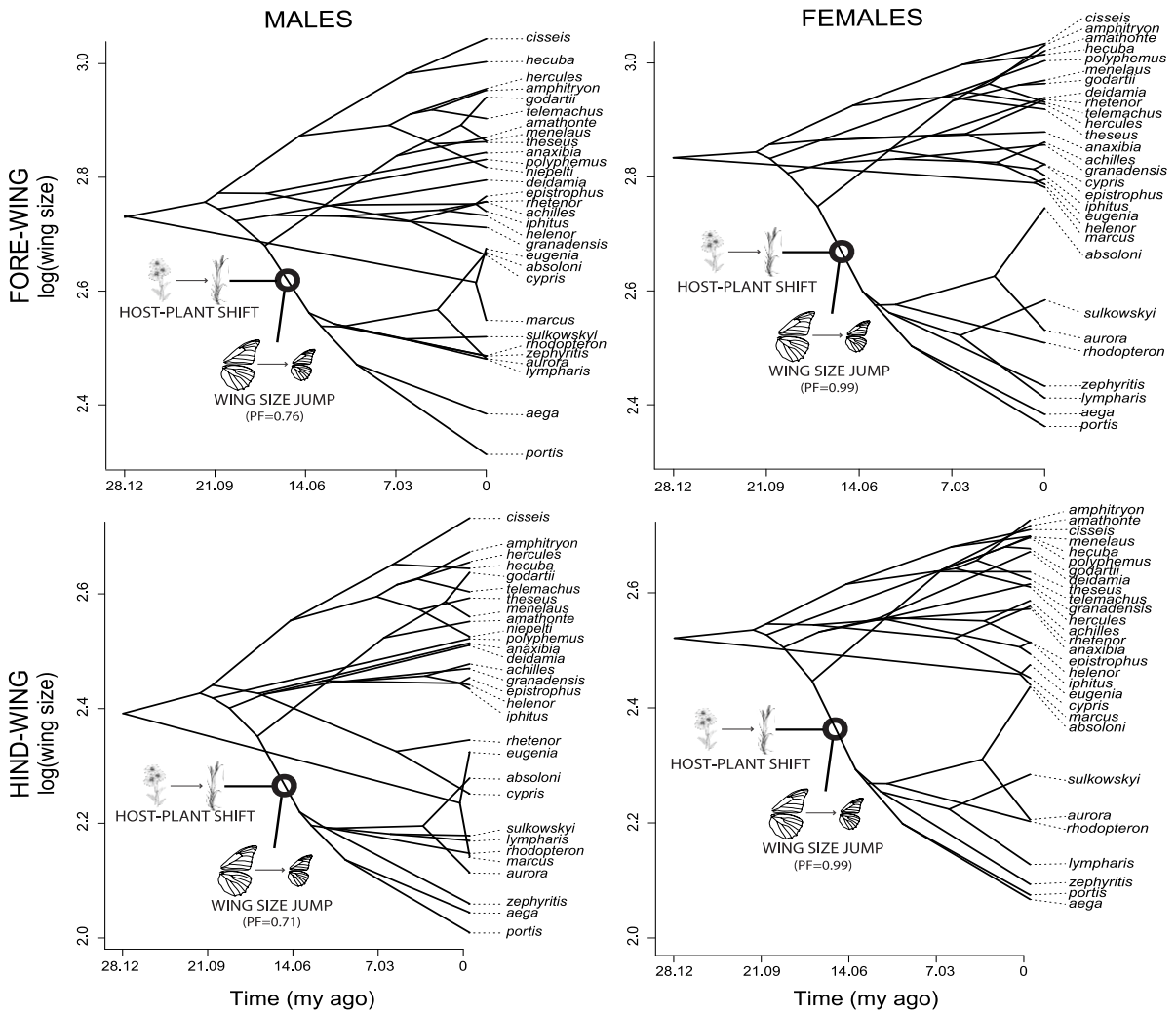

Figure 1. Phenograms for wing size (log scale) for males (left panels) and females (right panels). The top panels are the forewings, and the bottom panels are the hindwings. Wing size values are reconstructed at the nodes and plotted on a time scale. Phylogenetic relationships are projected into the phenogram. The position (branch) where the main host-plant shift and significant wing size jump happened is also shown. PF values indicate the frequency at which each jump was found across the posterior distribution of trees.

a) Males

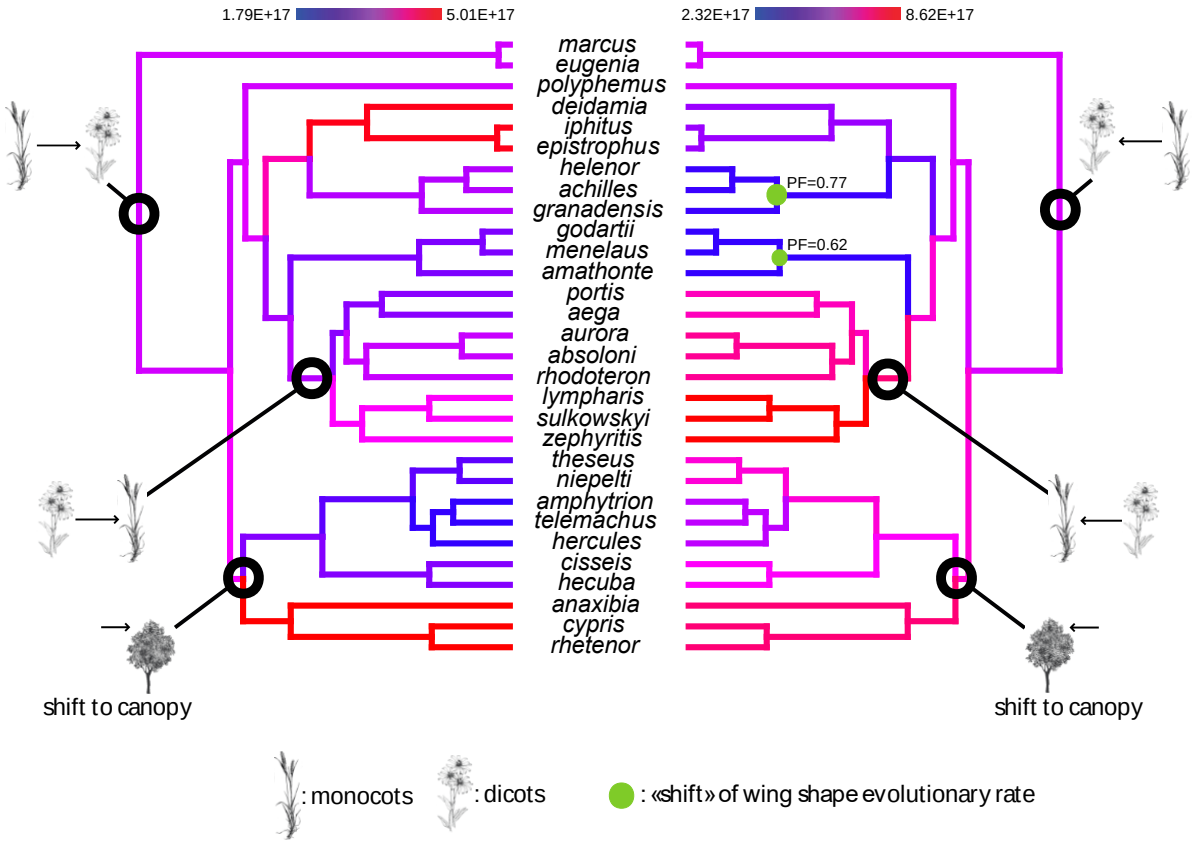

b) Females

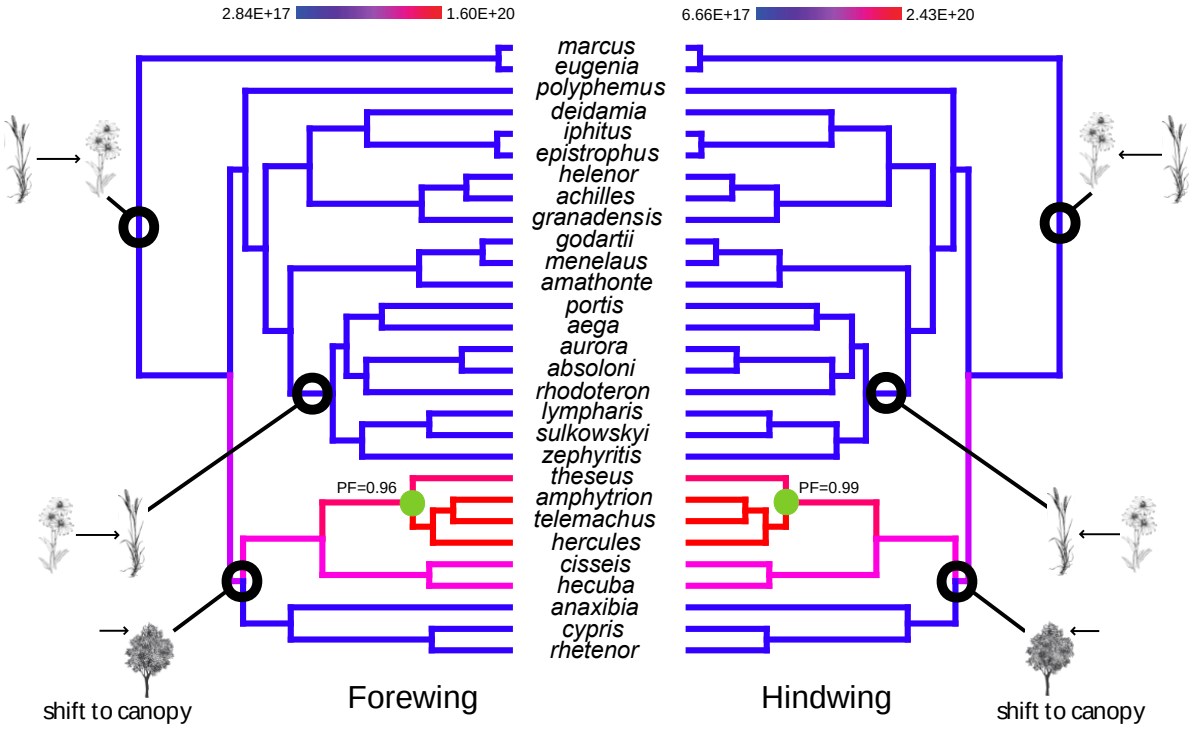

631 **Figure 2.** Rate of wing shape diversification for a) males and b) females. Branches of the
632 phylogenies are coloured according to the evolutionary rate inferred at the nodes using the R
633 package GEOMORPH. Green points indicate the changes in the rate of wing shape evolution
634 and black points the evolutionary jumps of wing size. Only shifts with a posterior tree
635 frequency higher than 0.5 are shown. PF values indicate the frequency at which each shift
636 was found across the posterior distribution of trees. On these phylogenies some major
637 evolutionary events including important host-plant shifts and microhabitat shifts are also
638 indicated.

639

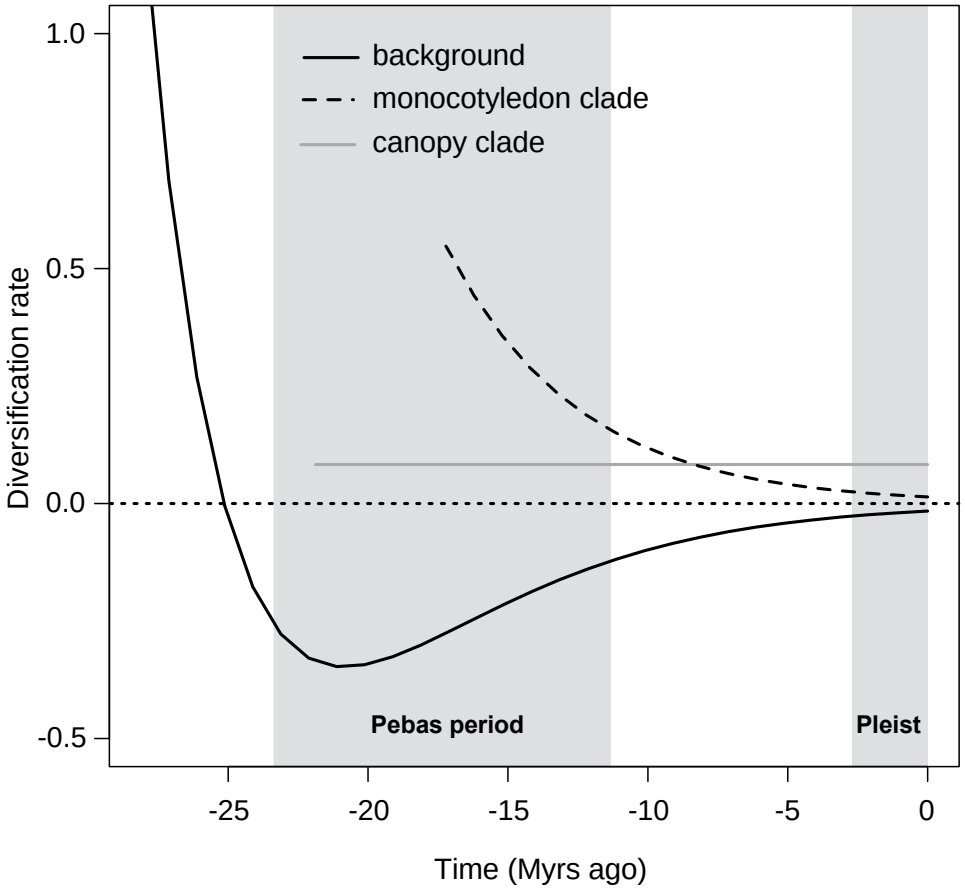

640

641 **Figure 3.** Estimation of the temporal dynamics of diversification for the genus *Morpho*.
642 Diversification rates (speciation minus extinction) for the best models identified for the
643 different subclades (canopy and monocotyledon) and the remaining lineages (background).
644 The early background diversification is elevated and decreases through time until it becomes
645 negative in the early Miocene. The canopy clade has constant rates of diversification, while
646 the monocotyledon clade conforms to an early-burst pattern with high rates that decrease
647 toward the present.
648

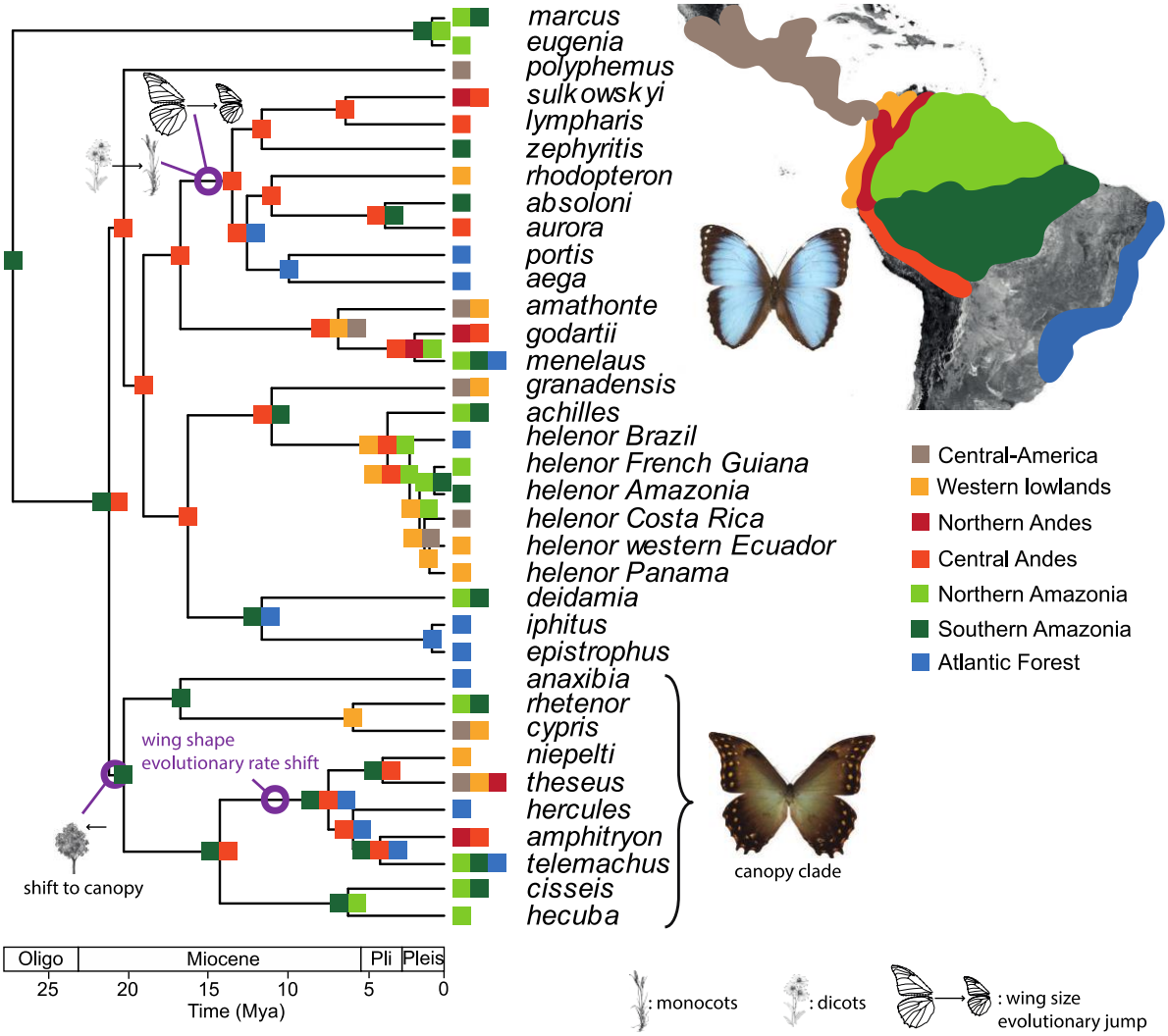

Figure 4. Historical biogeography inferred for the genus *Morpho*. The most likely states are indicated at the nodes. The different clade-specific ecological factors are also indicated on the tree. The two pictures of *Morpho* depict the typical wing shapes associated with each microhabitat – top: short rounded wings characteristic of the understory species, bottom: elongated wings toward the apex characteristic of the canopy clade.

REFERENCES

Adams D.C. (2014). Quantifying and comparing phylogenetic evolutionary rates for shape and other high-dimensional phenotypic data. *Systematic Biology*, 63, 166-177.

Antoine P.O., Abello M.A., Adnet S., Sierra A.J.A., Baby P., Billet G., Corfu F., … and R. Salas-Gismondi (2016). A 60-million-year Cenozoic history of western Amazonian ecosystems in Contamana, eastern Peru. *Gondwana Research* 31, 30-59.

Beaulieu J.M. and B.C. O'Meara. (2015). Extinction can be estimated from moderately sized molecular phylogenies. *Evolution*, 69, 1036-1043.

Beccaloni G.W., Viloria A.L., Hall S.K., and G.S. Robinson (2008). Catalogue of the hostplants of the Neotropical butterflies. Sociedad Entomológica Aragonesa. Monografias Tercer Milenio, 8, 1-536.

Blandin P. (2007). The systematics of the genus *Morpho* Fabricius, 1807. Hillside Books, Canterbury.

Blandin P. and B. Purser (2013). Evolution and diversification of Neotropical butterflies: Insights from the biogeography and phylogeny of the genus *Morpho* Fabricius, 1807 (Nymphalidae: Morphinae), with a review of the geodynamics of South America. *Tropical Lepidoptera Research*, 23, 62-85.

Cassildé C., Blandin P., Pierre J. and T. Bourgoin (2010). Phylogeny of the genus *Morpho* Fabricius, 1807, revisited (Lepidoptera, Nymphalidae). *Bulletin de la Société Entomologique de France*, 115, 225-250.

Cassildé C., Blandin P. and J.F. Silvain (2012). Phylogeny of the genus *Morpho* Fabricius 1807: insights from two mitochondrial genes (Lepidoptera: Nymphalidae). *Annales de la Société Entomologique de France*, 48, 173-188.

Chazot N., Panara S., Zilbermann N., Blandin P., Le Poul Y., Cornette R., Elias M. and V. Debat (2016). Morpho morphometrics: Shared ancestry and selection drive the evolution of wing size and shape in Morpho butterflies. *Evolution*, 70, 181-194.

Chazot N., Willmott K.R., de-Silva D.L., Condamine F., Morlon H., Freitas A.V.L., Uribe S., Giraldo-Sanchez C., Lamas G., Joron M., Jiggins C. and M. Elias (2016). Into the Andes:

683 Multiple colonisations and local diversification explain Andean diversity in the Godyridina
684 butterfly subtribe (Ithomiini). *Molecular Ecology*, 25, 5765-5784.
685 Chazot N., Willmott K.R., Lamas G., Freitas A.V.L., Piron-Prunier F., Arias C.F., De-Silva D.L. and
686 M. Elias (2018). Renewed diversification following Miocene landscape turnover in a
687 Neotropical butterfly radiation. Global Ecology and Biogeography, 28, 1118-1132.
688 Condamine F.L., Rolland J. and H. Morlon (2013). Macroevolutionary perspectives to environmental
689 change. *Ecology Letters*, 16, 72-85.
690 Condamine F.L., Antonelli A., Lagomarsino L.P., Hoorn C. and Liow L.H. (2018). Teasing apart
691 mountain uplift, climate change and biotic drivers of species diversification. In: Mountains,
692 Climate and Biodiversity (eds. Hoorn C., Perrigo A.L. & Antonelli A.). pp. 257-272. John
693 Wiley & Sons Ltd.
694 Constantino L.M. (1997). Natural history, immature stages and hostplants of *Morpho amathonte* from
695 western Colombia. *Tropical Lepidoptera*, 8, 75-80.
696 Cooney C. R. and Thomas G. H. (2021). Heterogeneous relationships between rates of speciation and
697 body size evolution across vertebrate clades. *Nature Ecology & Evolution*, 5, 101-110.
698 Denton J.S. and D.C. Adams (2015). A new phylogenetic test for comparing multiple
699 high-dimensional evolutionary rates suggests interplay of evolutionary rates and modularity in
700 lanternfishes (Myctophiformes; Myctophidae). *Evolution*, 69, 2425-2440.
701 De-Silva D.L., Elias M., Willmott K., Mallet J. and J.J. Day (2016). Diversification of clearwing
702 butterflies with the rise of the Andes. *Journal of Biogeography*, 43, 44-58.
703 De-Silva D.L., Mota L.L., Chazot N., Mallarino R., Silva-Brandão K.L., Piñerez L.M.G., Freitas
704 A.V.L., Lamas G., Joron M., Mallet J., Giraldo C.E., Uribe S., Särkinen T., Knapp S., Jiggins
705 C.D., Willmott K.R. and M. Elias (2017). Origin and diversification of the largest ithomiine
706 butterfly genus, *Pteronymia* Butler & Druce, 1872 (Lepidoptera: Nymphalidae), in the Northern
707 Andes. *Scientific Reports*, 7, 45966.
708 DeVries P.J., Penz C.M. and R.I. Hill (2010). Vertical distribution, flight behaviour and evolution of
709 wing morphology in *Morpho* butterflies. *J Anim Ecol*, 79, 1077-1085.

710 Drummond A.J., Suchard M.A., Xie D. and A. Rambaut (2012). Bayesian phylogenetics with BEAUti
711 and the BEAST 1.7. *Molecular Biology and Evolution*, 29, 1969-1973.
712 Dudley R. (2002). *The biomechanics of insect flight*. Princeton Univ. Press, Princeton, NJ.
713 Eastman J.M., Alfaro M.E., Joyce P., Hipp A.L. and L.J. Harmon (2011). A novel comparative
714 method for identifying shifts in the rate of character evolution on trees. *Evolution*, 65, 3578-
715 3589.
716 Elias M., Joron, M., Willmott K., Silva-Brandão K.L., Kaiser V., Arias C.F., Gomez Piñeres L.M.,
717 Uribe S., Brower A.V.Z., Freitas A.V.L. and C. Jiggins (2009). Out of the Andes: patterns of
718 diversification in clearwing butterflies. *Molecular Ecology*, 18, 1716-1729.
719 Evenstar L.A., Stuart F.L., Hartley A.J. and B. Tattitch (2015). Slow Cenozoic uplift of the western
720 Andean Cordillera indicated by cosmogenic ^{3}He in alluvial boulders from the Pacific Planation
721 Surface. *Geophysical Research Letter*, 42, 8448-8455.
722 Farris D.W., Jaramillo C. Bayona G., Restrepo-Moreno S.A., Montes C., Cardona A., Mora A.,
723 Speakman R.J., Glascock M.D. and V. Valencia (2011). Fracturing of the Panamanian Isthmus
724 during initial collision with South-America. *Geology*, 39, 1007-1010.
725 Fiorella R.P., Poulsen C.J., Pillco Zolá R.S., Barnes J.B., Tabor C.R. and T.A. Ehlers (2015).
726 Spatiotemporal variability of modern precipitation δ^{18}O in the central Andes and implications
727 for paleoclimate and paleoaltimetry estimates. *Journal of Geophysical Research: Atmospheres*,
728 120, 4630-4656.
729 Foote M. (1997). The evolution of morphological diversity. *Annual Review of Ecology and*
730 *Systematics*, 28, 129-152.
731 García-Barros E. (2000). Body size, egg size, and their interspecific relationships with ecological and
732 life history traits in butterflies (Lepidoptera: Papilionoidea, Hesperioidea). *Biological Journal*
733 *of the Linnean Society*, 70, 251-284.
734 Gavrilets S. and J. B. Losos (2009). Adaptive radiation: contrasting theory with data. *Science*, 323,
735 732-737.
736 Grodnitsky D.L., Dudley R. and L. Gilbert (1994). Wing decoupling in hovering flight of swallowtail
737 butterflies (Lepidoptera: Papilionidae). *Tropical Lepidoptera*, 5, 85-86.

738 Harmon L.J., Weir J., Brock C., Glor R.E. and W. Challenger (2008). GEIGER: Investigating
739 evolutionary radiations. *Bioinformatics*, 24, 129-131.
740 Hoorn C., Wesselingh F.P., ter Steege H., Bermudez M.A., Mora A., Sevink J., Sanmartín I.,
741 Sanchez-Meseguer A., Anderson C.L., Figueiredo J.P., Jaramillo C., Riff D., Negri F.R.,
742 Hooghiemstra H., Lundberg J., Stadler T., Sarkinen T. and A. Antonelli (2010). Amazonia
743 through time: andean uplift, climate change, landscape evolution, and biodiversity. *Science*,
744 330, 927-931.
745 Janz N., Nylin S. and N. Wahlberg (2006). Diversity begets diversity: host expansions and the
746 diversification of plant-feeding insects. *BMC Evolutionary Biology*, 6, 4.
747 Lagomarsino L.P., Condamine F.L., Antonelli A., Mulch A. and C.C. Davis (2016). The abiotic and
748 biotic drivers of rapid diversification in Andean bellflowers (Campanulaceae). *New Phytologist*,
749 210, 1430-1442.
750 Lanfear R., Calcott B., Ho S.Y.W. and S. Guindon (2012). PartitionFinder: combined selection of
751 partitioning schemes and substitution models for phylogenetic analyses. *Molecular Biology and*
752 *Evolution*, 29, 1695-1701.
753 Langerhans R.B., Anderson C. M. and J. L. Heinen-Kay (2016). Causes and consequences of genital
754 evolution. *Integrative and Comparative Biology*, 56, 741-751.
755 Lee M.S., Sanders K.L., King B. and A. Palci (2016). Diversification rates and phenotypic evolution
756 in venomous snakes (Elapidae). *Royal Society Open Science*, 3, 150.
757 Leier A., McQuarrie N., Garzione C. and J. Eiler (2013). Stable isotope evidence for multiple pulses
758 of rapid surface uplift in the Central Andes, Bolivia. *Earth and Planetary Science Letters*, 371,
759 49-58.
760 Le Roy C., Cornette R., Llaurens V. and Debat V. (2019). Effects of natural wing damage on flight
761 performance in Morpho butterflies: what can it tell us about wing shape evolution? *Journal of*
762 *Experimental Biology*, 222, xxx-yyy.
763 Le Roy C., Debat V. and Llaurens, V. (2019). Adaptive evolution of butterfly wing shape: from
764 morphology to behaviour. *Biological Reviews*, 94, 1261-1281.

765 Matzke N.J. (2014). Model selection in historical biogeography reveals that founder-event speciation
766 is a crucial process in island clades. *Systematic Biology*, 63, 951-970.
767 Merrill R.M., Chia A. and N.J. Nadeau (2014). Divergent warning patterns contribute to assortative
768 mating between incipient *Heliconius* species. *Ecology & Evolution*, 4, 911–917.
769 Montes C., Cardona A., McFadden R., Morón S.E., Silva C.A., Restrepo-Moreno S., Ramírez D.A.,
770 Hoyos N., Wilson J., Farris D., Bayona G.A., Jamarillo C.A., Valencia V., J. Bryan and J.A.
771 Flores (2012). Evidence for middle Eocene and younger land emergence in central Panama:
772 implications for Isthmus closure. *Geol Soc Am Bull*, 124, 780-799.
773 Morlon H., Parsons T.L. and J.B. Plotkin (2011). Reconciling molecular phylogenies with the fossil
774 record. *Proceedings of the National Academy of Sciences of the U.S.A.*, 108, 16327-16332.
775 Naisbit R.E., Jiggins C.D. and J. Mallet (2001). Disruptive sexual selection against hybrids
776 contributes to speciation between *Heliconius cydno* and *Heliconius melpomene*. *Proceedings of*
777 *the Royal Society of London B: Biological Sciences*, 268, 1849-1854.
778 Ortiz-Acevedo E., Gomez J. P., Espeland M., Toussaint, E. F. and Willmott K. R. (2020). The roles of
779 wing color pattern and geography in the evolution of Neotropical Preponini butterflies. *Ecology*
780 *and Evolution*, 10, 12801-12816.
781 Plummer M., Best N., Vines K., Sarkar D., Bates D., Almond R., Magnusson A. (2020). coda:
782 Output Analysis and Diagnostics for MCMC. R CRAN respository, https://cran.r-
783 project.org/web/packages/coda/index.html
784 Penz C.M., Devries P.J. and N. Wahlberg (2012). Diversification of Morpho butterflies (Lepidoptera,
785 Nymphalidae): a re-evaluation of morphological characters and new insight from DNA
786 sequence data. *Systematic Entomology*, 37, 670-685.
787 Price S.A., Claverie T., Near T.J. and P.C. Wainwright (2015). Phylogenetic insights into the history
788 and diversification of fishes on reefs. *Coral Reefs*, 34, 997-1009.
789 Quental, T. B. and Marshall, C. R. (2010). Diversity dynamics: molecular phylogenies need the fossil
790 record. *Trends in Ecology & Evolution*, 25, 434-441.
791 Rabosky D.L. (2010). Extinction rates should not be estimated from molecular phylogenies.
792 *Evolution*, 64, 1816-1824.
793 Rabosky D.L. and Adams DC. (2012). Rates of morphological evolution are correlated with species
794 richness in salamanders. *Evolution*, 66, 1807-1818.

795 Rabosky D.L., Santini F., Eastman J.M., Smith S.A., Sidlauskas B., Chang J. and Alfaro M.E. (2013).
796 Rates of speciation and morphological evolution are correlated across the largest vertebrate
797 radiation. *Nature Communications*, 4, 2958.
798 Rabosky R.D., Donnellan S.C., Grundler M. and I. Lovette (2014). Analysis and visualization of
799 complex macroevolutionary dynamics: an example from Australian scincid lizards. *Systematic*
800 *Biology*, 63, 610-627.
801 Ree R.H. and S.A. Smith (2008) Maximum likelihood inference of geographic range evolution by
802 dispersal, local extinction, and cladogenesis. *Systematic Biology*, 57, 4-14.
803 Revell L.J. (2012) phytools: An R package for phylogenetic comparative biology (and other things).
804 *Methods in Ecology & Evolution*, 3, 217-223.
805 Salas-Gismondi R., Flynn J.J., Baby P., Tejada-Lara J.V., Wesselingh F.P. and P.O. Antoine (2015).
806 A Miocene hyperdiverse crocodylian community reveals peculiar trophic dynamics in proto-
807 Amazonian mega-wetlands. *Proceedings of the Royal Society of London B: Biological*
808 *Sciences*, 282, 20142490.
809 Sauquet H., Ho S.Y., Gandolfo M.A., Jordan G.J., Wilf P., Cantrill D.J., Bayly M.J., Bromham L.,
810 Brown G.K., Carpenter R.J., Lee D.M., Murphy D.J., Sniderman J.M. and F. Udovicic (2011).
811 Testing the impact of calibration on molecular divergence times using a fossil-rich group: the
812 case of *Nothofagus* (Fagales). *Systematic Biology*, 61, 289-313.
813 Schluter D. (2000). *Ecology of adaptive radiation.* Oxford: Oxford University Press.
814 Thacker C.E. (2014). Species and shape diversification are inversely correlated among gobies and
815 cardinalfishes (Teleostei: Gobiiformes). *Org Divers Evol*, 14, 419-436.
816 Uyeda J.C., Caetano D.S. and M.W. Pennell (2014). Comparative analysis of principal components
817 can be misleading. *Systematic Biology*, 64, 677-689.
818 Vásquez Bardales J., Zárate Gómez R., Huiñapi Canaquiri P., Pinedo Jiménez J., Ramírez Hernández
819 J. J., Lamas G., and Vela García P. (2017). Plantas alimenticias de 19 especies de mariposas
820 diurnas (Lepidoptera) en Loreto, Perú. *Revista peruana de biología*, 24(1), 35-42.
821 Venditti C., Meade A. and M. Pagel (2011). Multiple routes to mammalian diversity. *Nature*, 479,
822 393-396.

823 Wahlberg N., Leneveu J., Kodandaramaiah U., Peña C., Nylin S., Freitas A.V.L. and A.V.Z. Brower
824 (2009). Nymphalid butterflies diversify following near demise at the Cretaceous/Tertiary
825 boundary. *Proceedings of the Royal Society of London B: Biological Sciences*, 276, 4295-4302.
826 Wesselingh F.P., Räsänen M.E., Irion G., Vonhof H.B., Kaandorp R., Renema W., Romero Pittman
827 L. and M. Gingras (2001). Lake Pebas: a palaeoecological reconstruction of a Miocene, long-
828 lived lake complex in western Amazonia. *Cainozoic Research*, 1, 35-68.
829 Zachos J.C., Dickens G.R. and R.E. Zeebe (2008). An early Cenozoic perspective on greenhouse
830 warming and carbon-cycle dynamics. *Nature*, 451, 279-283.
831 Zelditch M.L., Li J., Tran L.A. and D.L. Swiderski (2015). Relationships of diversity, disparity, and
832 their evolutionary rates in squirrels (Sciuridae). *Evolution*, 69, 1284-1300.